Research Square

Preprints are preliminary reports that have not undergone peer review. They should not be considered conclusive, used to inform clinical practice, or referenced by the media as validated information.

Identification and Characterization of Ovarian Extrachromosomal Circular Deoxyribonucleic Acid in Rats with Polycystic Ovary Syndrome

Zhi Chen
Chongqing Traditional Chinese Medicine Hospital
Hao Song
Chongqing Medical University
Jun-jie Deng
Chongqing Medical University
Yuan-xue Wu
Chongqing Medical University
Tian-jiao Liu
Chengdu Women's and Children's Central Hospital
Min Xia
Chongqing Traditional Chinese Medicine Hospital
Ao-lei Lin
Tianjin Medical University General Hospital
Cheng Chen
Chongqing General Hospital
Jun-yu Feng
Chongqing Traditional Chinese Medicine Hospital
Huan Yang
yanghuan@sxzxyy.cn

Chongqing University Three Gorges Hospital

Research Article

Keywords: eccDNAs/ecDNAs, PCOS, Circle-seq, Rat ovaries

Posted Date: July 16th, 2026

DOI: https://doi.org/10.21203/rs.3.rs-10280475/v1

License: This work is licensed under a Creative Commons Attribution 4.0 International License.
Read Full License

Additional Declarations: No competing interests reported.

Abstract

Objective: To characterize the expression profile of extrachromosomal circular deoxyribonucleic acid in polycystic ovary syndrome ovaries and elucidate their potential functions and interactions with non-coding ribonucleic acids and circular ribonucleic acids.

Design: An experimental study using a polycystic ovary syndrome rat model combined with high-throughput sequencing and bioinformatics analysis.

Subjects: Female Sprague-Dawley rats randomly assigned to control and polycystic ovary syndrome groups.

Exposure: Polycystic ovary syndrome was induced via subcutaneous injection of dehydroepiandrosterone for 21 consecutive days.

Main Outcome Measures: Follicular development assessed by hematoxylin-eosin staining; serum sex hormones measured by enzyme-linked immunosorbent assay; estrous cycles monitored by light microscopy; extrachromosomal circular deoxyribonucleic acid profiles determined by circle sequencing; host gene functions and pathways analyzed by gene ontology and pathway enrichment analysis; extrachromosomal circular deoxyribonucleic acid presence confirmed by transmission electron microscopy; differential expression validated by gel electrophoresis.

Results: Polycystic ovary syndrome rats exhibited abnormal follicular development, disrupted sex hormone levels, and irregular estrous cycles. A total of 15,207 extrachromosomal circular deoxyribonucleic acid molecules representing 13,762 distinct types were identified, with significantly lower abundance in the polycystic ovary syndrome group. Among 263 differentially expressed extrachromosomal circular deoxyribonucleic acid molecules, all were small circular deoxyribonucleic acids. Length distribution showed a unimodal pattern in controls peaking at 368 base pairs versus a bimodal pattern in polycystic ovary syndrome with peaks at 212 base pairs and 359 base pairs. Extrachromosomal circular deoxyribonucleic acid originated widely from various chromosomes without significant intergroup differences, predominantly from gene-enriched regions with 4-20 base pair repeats at junctions. No significant guanine-cytosine content differences were observed. Host genes partially or completely overlapped with non-coding ribonucleic acids, transposable elements, and circular ribonucleic acids. Functional analysis revealed enrichment in synaptic structure, signal transmission, iron ion homeostasis, and cell junction formation. Pathway analysis indicated T cell receptor signaling pathway enrichment. Transmission electron microscopy confirmed ovarian extrachromosomal circular deoxyribonucleic acid presence, and gel electrophoresis validated differential expression.

Conclusion: This study first reveals the extrachromosomal circular deoxyribonucleic acid expression profile in polycystic ovary syndrome ovaries, clarifies their functions, and elucidates synergistic mechanisms with non-coding ribonucleic acids and circular ribonucleic acids, providing novel insights

into polycystic ovary syndrome pathogenesis and potential diagnostic biomarkers and therapeutic targets.

1. Introduction

PCOS is a common gynecological endocrine disorder primarily characterized by hyperandrogenism, insulin resistance, hirsutism, acne, and menstrual irregularities(1–3). With a prevalence of approximately 4%-20% among women of reproductive age, PCOS affects a large patient population and is one of the leading causes of ovulatory infertility(4) In recent years, the incidence of PCOS has been steadily rising, imposing significant physiological, psychological, and economic burdens on patients while adversely affecting their quality of life(5).

Extensive research indicates that PCOS arises from complex gene-environment interactions, with endocrine disruption at its core, though its precise pathogenesis remains unclear(6). Studies suggest that endocrine disruptors like bisphenol A and obesity-related lifestyles exacerbate PCOS by interfering with hormonal homeostasis or intensifying metabolic imbalances; local ovarian dysfunction, including elevated theca cell androgen synthase activity and granulosa cell dysfunction, directly leads to follicular arrest and polycystic-like changes(7). These mechanisms intertwine to form a vicious cycle of “insulin resistance-hyperinsulinemia-hyperandrogenism-ovulatory dysfunction,” ultimately resulting in the characteristic pathological manifestations of PCOS.

EccDNAs/EcDNAs are circular DNA molecules that exist independently of chromosomes(8). Their core characteristic is homology with chromosomal DNA, meaning they originate from specific regions of the host genome, such as genes, regulatory elements, or repetitive sequences(9). Their lengths range from several hundred to millions of base pairs. Some studies classify eccDNAs/ecDNAs based on size, designating smaller ones as eccDNAs(10) and larger ones as ecDNAs(11). The formation mechanisms of eccDNAs/ecDNAs involve multiple pathways that remain incompletely understood. These include new formation mediated by microhomologous end-joining (MMEJ) or non-homologous end-joining (NHEJ) during DNA damage repair following chromosomal breaks or replication stress, and self-ligation of single-strand breaks triggered by replication errors such as DNA slippage or R-loop structures. They are widely present in mammalian eukaryotic cells and exhibit tissue specificity(12). Studies indicate that eccDNAs/ecDNAs are not only prevalent in tumor cells, such as those in ovarian and lung cancers, but are also expressed in human plasma, bone tissue, and the anterior capsule of the lens(13). However, their specific functions require further investigation.

EccDNAs/EcDNAs are extensively involved in the development and progression of both tumorous and non-tumorous diseases. For instance, eccDNAs/ecDNAs can drive tumor heterogeneity and drug resistance by harboring amplified oncogenes(14–16). Furthermore, Dutta et al. demonstrated that eccDNAs can regulate small RNAs to control gene expression in a promoter-independent manner(17). Abnormal copy numbers or transcriptional dysregulation of bone metabolism genes carried by eccDNAs can disrupt osteoblast-osteoclast balance, ultimately leading to age-related osteoporosis(18). Abnormal

copies of lens protein-related genes in eccDNAs may cause scleral fiber disorganization and lens opacity(15). Overexpression of eccDNA in placental tissue can impair placental material exchange, contributing to fetal growth restriction(19).

However, no reports have yet been published on the relationship between eccDNAs/ecDNAs and PCOS. Studies indicate that eccDNAs are widely expressed in ovarian tissue, where they regulate functions such as granulosa cell proliferation, hormone synthesis, and follicular development. Impaired ovarian follicular development and dysfunction are key pathological features of PCOS. Our preliminary findings revealed extensive expression of eccDNAs/ecDNAs in ovarian tissue, with downregulated expression observed in PCOS rats. Consequently, we hypothesize that eccDNAs/ecDNAs may mediate the pathogenesis and progression of PCOS. This study employs Circle-Seq sequencing technology to identify the expression profile of extrachromosomal circular DNA in ovarian tissues from both control and PCOS groups. We further investigate the expression profile, characteristics, and functions of eccDNAs/ecDNAs in PCOS ovarian tissue to explore their regulatory relationship with PCOS pathogenesis. Validation via PCR and Southern blotting confirms the presence of ecDNAs in ovaries. Our findings provide unprecedented insights into the existence of these enigmatic molecules in PCOS rat ovaries, bridging a gap in ecDNA/eccDNA research related to PCOS pathogenesis and offering novel perspectives for future studies.

2. Materials and methods

2.1 Animal Experiments and Establishment of the PCOS Rat Model

All animal procedures were approved by the Ethics Committee of Chongqing Hospital of Traditional Chinese Medicine (Approval No. 2022-DWSY-CZ) and conducted in accordance with the 3Rs principle (Replacement, Reduction, and Refinement) and relevant ethical guidelines for animal research. The PCOS rat model was established following previously published methods(18). Three-week-old female Sprague-Dawley rats were housed 3–5 per cage under standard laboratory conditions (12-hour light/12-hour dark cycle) with free access to food and water. The rats were randomly assigned to either the control group (n = 6) or the PCOS group (n = 6).

From day 21 to day 42, the PCOS group received a daily subcutaneous injection of dehydroepiandrosterone (DHEA, 6 mg/100 g body weight, dissolved in 0.2 ml sesame oil) to induce the PCOS model. The control group was injected with an equal volume of sesame oil using the same protocol. After 21 days of treatment, all animals underwent estrous cycle assessment, serum collection, and euthanasia, followed by ovarian collection and histopathological examination(20).

2.2 Ovarian Morphological Analysis

Ovarian morphology was evaluated by hematoxylin and eosin (H&E) staining, following our previously published protocol(11). Briefly, ovarian tissues were fixed overnight in 4% formaldehyde at room

temperature, dehydrated in graded ethanol, and embedded in paraffin. The paraffin blocks were sectioned at 4 μm thickness, deparaffinized, and rehydrated through graded alcohols. The sections were stained with H&E (Servicebio Technology Co., Ltd, Wuhan, China). Stained sections were examined under a light microscope (NIKON DS-U3, Nikon, Japan) for histological evaluation.

2.3 Serum Hormone Determination

After isoflurane anesthesia, blood samples were collected from the abdominal aorta and centrifuged at 3000 × g for 15 minutes at room temperature to obtain serum. Serum levels of follicle-stimulating hormone (FSH), luteinizing hormone (LH), testosterone (T), estradiol (E2), and insulin (INS) were measured using commercial ELISA kits (Elabscience Biotechnology Co., Ltd, Wuhan, China) according to the manufacturer's instructions. The catalog numbers for the kits were: FSH (E-EL-R0391c), LH (E-EL-R0026c), E2 (E-EL-0152c), INS (E-EL-R3034), and T (E-EL-0155c). Data were analyzed using Prism software (version 9.0, GraphPad Software, La Jolla, CA, USA).

2.4 Determination of Estrous Cycle

Estrous cyclicity was assessed by light microscopy in accordance with previously described methods. Vaginal smears were collected daily from day 32 to day 39 of the experimental period to evaluate the predominant cell populations. Estrous cycle stages were determined based on cytological characteristics as follows: proestrus, predominance of nucleated epithelial cells; estrus, presence of cornified squamous epithelial cells; metestrus, a mixture of cornified epithelial cells and leukocytes; and diestrus, predominance of leukocytes.

2.5 Library Construction and Sequencing

2.5.1 Elimination of Linear DNA and Enrichment of Circular DNA

A total of 1.5–2 μg of DNA was digested in a 100 μL reaction system using Plasmid-Safe ATP-Dependent DNase (Biosearch, E0054) at 37°C for 24 hours. Following this, DNase and ATP were added, and digestion was continued for at least 5 days until completion. The enrichment efficiency and quality of eccDNAs/ecDNAs were assessed by PCR using specific primers. PCR results were used to confirm the complete removal of linear DNA. High molecular weight (HMW) DNA produced target amplicons, whereas no amplification was observed after the complete digestion of linear DNA, confirming its elimination and indicating that the remaining DNA consisted of eccDNAs/ecDNAs.

In accordance with the manufacturer's instructions, enriched eccDNA samples were amplified using phi29 DNA polymerase (VAZYME, N106) and random hexamer primers. The phi29-amplified DNA products were then fragmented to an average size of 200–500 bp using a Bioruptor™ ultrasonicator (Diagenode). The resulting fragments were purified with the MolPure® Gel Extraction Kit (YEASEN, 19101).

2.5.2 Library Preparation and Sequencing

Libraries were prepared using the VAHTS Universal DNA Library Prep Kit for Illumina V3 (ND607) following the manufacturer's protocol, which includes end-repair, adapter ligation, size selection (200–500 bp), and PCR amplification. Final libraries were purified, assessed on an Agilent 2100 Bioanalyzer, and sequenced on an Illumina NovaSeq 6000 platform (paired-end 150 bp; 6–10 Gb per sample).

2.5.3 Read Processing and Alignment

Raw FASTQ reads were quality-checked using FastQC v0.11.9, and low-quality reads were removed. Clean reads were aligned to the Rattus norvegicus reference genome (rn6) using Burrows-Wheeler Aligner (BWA v0.7.17). Sorted SAM files were processed by Samtools v1.3.1 to produce BAM files for downstream analysis.

2.6 Identification and Annotation of EccDNAs/EcDNAs

EccDNAs/EcDNAs were detected using Circle-Map(14). The genome was divided into functional regions, including the 5' UTR, exons, introns, 3' UTR, ± 2 kb gene flanks, CpG islands, transposable elements (TEs), and B1/B2/ID elements. Circular DNAs were annotated using BEDTools, and those overlapping coding regions were defined as eccDNA/EcDNA-associated genes. Shared and unique genes among groups were compared, and their distribution was visualized as bar plots.

2.7 Abundance and Differential Expression Analysis

Read counts for each eccDNA/EcDNA were computed using FeatureCounts, normalized by DESeq2, and visualized through principal component analysis (PCA) in R. Differentially expressed eccDNAs between PCOS and control ovaries were identified by DESeq2 with $|\log_2 FC| > 1$ and $p < 0.05$.

2.8 Functional Enrichment of EccDNA/EcDNA-Associated Genes

Genes associated with differentially expressed eccDNAs/ecDNAs were subjected to GO and KEGG enrichment analyses using the ClusterProfiler R package, to elucidate their biological functions and the pathways in which they are involved.

2.9 Junctional Motif Analysis

The ± 20 bp flanking sequences of eccDNA/EcDNA junctions were extracted, and 4–20 bp direct or inverted repeat motifs were identified using R v3.4.2 and clusterProfile for visualization and statistical evaluation.

2.10 GC Content Analysis

GC content was measured for three regions: the start-to-end region, the start junction site (from start to start − 100 bp), and the end junction site (from end to end + 100 bp). Histograms were generated to visualize the data, and paired t-tests were used to analyze differences between groups.

2.11 Association of Circular DNA With Transposable Elements and ncRNAs

To examine overlaps among circular DNA, transposable elements (TEs), and non-coding RNAs (ncRNAs), the genomic coordinates of lncRNAs, miRNAs, snoRNAs, and tRNAs were obtained from Ensembl (rn6 GTF) and compared with eccDNA/EcDNA loci using BEDTools and BLAST. TE annotations were downloaded from the UCSC RepeatMasker database. The lncRNA category included antisense, intronic, and processed transcripts; ncRNAs comprised lncRNAs, snoRNAs, and mitochondrial tRNAs (Mt_tRNAs).

2.12 Experimental Verification

Total DNA from ovarian tissue was extracted using the SteadyPure Genomic DNA Extraction Kit (Aikery Biotech), and circular DNAs were enriched following the reported Circle-Seq protocol. Briefly, ovarian tissues were pulverized under liquid nitrogen, followed by cell lysis, DNA purification, and enzymatic removal of linear DNA to obtain enriched eccDNA fractions for downstream analyses.

Based on eccDNA sequencing results, four eccDNAs showing significant intergroup differences were randomly selected as representative candidates for experimental validation. These eccDNAs were designated in a neutral and sequential manner as eccDNA001–eccDNA004 to avoid functional presupposition. Validation was performed by PCR using outward-facing primers specific to each circular DNA, enabling selective amplification across the circular junctions. Primer sequences are listed in Supplementary Table 1.

PCR amplification was performed using a SYBR Green Pro Taq HS Premix qPCR Kit (Aikery Biotech) with total ovarian DNA as the template. Each 20 μL reaction contained 10 μL 2× SYBR Green Pro Taq HS Premix, 2 μL DNA template (100 ng), 0.4 μL of each primer, and 7.2 μL nuclease-free water. PCR products were resolved on a 1% agarose gel prepared in 1× TAE buffer supplemented with SerRed nucleic acid dye and visualized after electrophoresis at 120 V for 35 minutes.

2.13 Statistical Analysis

Statistical analyses were performed using SPSS 26.0, with significance set at $P = 0.05$. Data are presented as mean ± standard deviation (± SD). Independent sample t-tests were used to assess statistical significance, with $p < 0.05$ considered significant.

3. Result

3.1 Establishment and validation of the PCOS rat model

Hematoxylin and eosin (H&E) staining revealed marked ovarian morphological differences between the control and PCOS groups. Control ovaries displayed follicles at various developmental stages and abundant corpora lutea, whereas PCOS ovaries exhibited multiple cystic follicles with a pronounced

reduction in corpora lutea. Quantitative analysis confirmed a significant decrease in the number of corpora lutea and a significant increase in cystic follicles in the PCOS group (Fig. 1A).

Estrous cycle monitoring showed regular cyclicity in control rats, while PCOS rats remained predominantly in the diestrus stage throughout the observation period, indicating disrupted ovarian cyclicity (Fig. 1B). Serum hormone analysis demonstrated significant endocrine alterations in PCOS rats, including elevated testosterone and luteinizing hormone (LH) levels and reduced insulin (INS) levels. No significant differences were observed in follicle-stimulating hormone (FSH) or estradiol (E2) levels between the groups (Fig. 1C).

3.2. Quantification of eccDNAs/ecDNAs

Through collection, purification, and enrichment steps, eccDNAs/ecDNAs were isolated from the samples in four stages **(Supplementary Fig. 1)**. A total of 15,207 eccDNAs/ecDNAs were detected across six ovarian tissues, including 14,977 eccDNAs and 230 ecDNAs (Fig. 2A). Specifically, the control group identified 202 ecDNAs and 13,569 eccDNAs (Fig. 2B), while the PCOS group revealed 112 ecDNAs and 2,769 eccDNAs (Fig. 2C).

We further observed that the number of eccDNAs in the PCOS group (431 ± 299; n = 3) (P = 0.004) was significantly lower than that in the control group (2,021 ± 365.5; n = 3). Conversely, the number of ecDNAs in the PCOS group (47.00 ± 4.163; n = 3) was also lower than in the control group (73.67 ± 7.767; n = 3, P = 0.012) (Fig. 2D).

To further investigate the characteristics of eccDNAs/ecDNAs, we identified the types of eccDNAs, revealing 12,208 eccDNAs types and 118 ecDNAs types in the control group (Fig. 2E), while the PCOS group contained 1,408 eccDNAs types (Fig. 2G) and 28 ecDNAs types (Fig. 2F). As shown in Figure H, the total number of unique eccDNA+ecDNA was significantly decreased in the PCOS group compared with the Control group (1715.3 ± 411.6 vs. 195.3 ± 311.5, P < 0.01). Consistently, unique ecDNA counts were markedly reduced in PCOS ovaries (1684.3 ± 412.9 vs. 189.7 ± 311.2, P < 0.001). In addition, unique eccDNA was also significantly lower in the PCOS group than in Controls (31.0 ± 3.6 vs. 5.7 ± 3.5, P < 0.01). (Fig. 2H)Venn diagram analysis revealed 1,361 overlapping eccDNAs and 84 overlapping ecDNAs between the two groups (Fig. 2I-2J).

3.3. Chromosomal Origins of eccDNAs/ecDNAs

We identified a substantial number of eccDNAs/ecDNAs, yet their chromosomal origins remain unclear. To investigate whether the chromosomal origins of eccDNAs/ecDNAs exhibit any preferences, we statistically analyzed their chromosomal sources. Our results indicate that the chromosomal origins of eccDNAs/ecDNAs in the PCOS group significantly differ from those in the control group, exhibiting substantial intergroup heterogeneity. The vast majority of eccDNAs/ecDNAs in both groups originate from autosomes, with a smaller proportion derived from sex chromosomes. Chromosome 1 contributes the highest number of eccDNAs/ecDNAs (Fig. 3A).

Additionally, we quantified the eccDNAs density distribution per megabase across each chromosome. In contrast, the control group exhibited markedly higher eccDNAs density on chromosomes 12, 10, and 19 relative to the PCOS group. Notably, the eccDNAs density per Mb on chromosome 12 was significantly higher than on other chromosomes in both groups (Fig. 3B).

3.4 Size Analysis of eccDNAs/ecDNAs

To investigate size distribution differences between identified eccDNAs/ecDNAs in the Control and PCOS groups, we plotted their length distributions. The results revealed that eccDNA sizes in both groups exhibited a bimodal normal distribution pattern (Fig. 4A), with peaks concentrated around 0.6 kb. In contrast, ecDNA displayed a broad columnar distribution without significant clustering peaks, showing greater fragmentation and dispersion in length distribution (Fig. 4B).

Additionally, we performed length distribution statistics for both groups of ovarian eccDNAs/ecDNAs, with both yielding bimodal distributions (Fig. 4C). To determine whether pathological factors influence circular DNA fragment size, we plotted length distribution density plots and cumulative distribution plots for eccDNA, comparing the length distributions between the two groups. Results revealed two distinct peaks in the PCOS group at 212 bp and 359 bp, whereas the control group exhibited peaks at 208 bp and 368 bp. The average length of eccDNAs/ecDNAs in the control group was significantly longer than that in the PCOS group (Fig. 4D).

The cumulative distribution plot revealed that eccDNAs predominantly clustered within the 0 bp to 4000 bp range, exhibiting a marked ascending trend between 0 and 1500 bp.

3.5 Expression Patterns of eccDNAs/ecDNAs

To investigate the similarity between the two sample groups, we PCA based on the eccDNAs/ecDNAs within each sample. The PCA results revealed that the PCOS group exhibited higher sample similarity than the control group, both in ecDNAs **(Supplementary Fig. 2A)** and eccDNAs **(Supplementary Fig. 2B)**.

Using a 2-fold change and P = 0.05 between the two sample groups, we identified a total of 263 DEEECs/DEECs, comprising 260 DEEECs and 3 DEECs, including 226 downregulated and 37 upregulated DEEECs/DEECs. Heatmap analysis displayed representative differentially expressed eccDNAs (Fig. 5A) and ecDNAs (Fig. 5B). A volcano plot shows the 226 downregulated and 37 upregulated DEEECs/DEECs (Fig. 5C).

3.6 Genomic Annotation of eccDNAs/ecDNAs

To elucidate the origins of circular DNA and explore the relationship between circular DNA sources and host genes, we compared the sequences of eccDNAs/ecDNAs with their corresponding host gene sequences. The results showed that the identified eccDNAs predominantly originated from intronic and intergenic regions of host genes, with a smaller proportion derived from exonic regions, as well as the upstream and downstream 2 kb flanking regions of genes. These findings indicate that the generation of

eccDNAs exhibits clear regional preferences within the genome (Fig. 6A). In contrast, ecDNAs primarily originated from exons, introns, and intergenic regions **(Supplementary Fig. 3A)**, highlighting marked differences in the genomic sources of eccDNAs and ecDNAs.

To further delineate which regions of the host genome contribute to eccDNAs/ecDNAs, host genes were subdivided into 12 detailed genomic segments. We found that eccDNAs mainly originated from coding regions, introns, and transposable elements (TEs) within host genes (Fig. 6B). By comparison, ecDNAs were derived from all regions of host genes, with the highest abundance arising from TEs **(Supplementary Fig. 3B)**.

To clarify the contribution of direct and inverted repeat sequences to eccDNAs/ecDNAs formation in PCOS rat ovaries, BLAST analysis was performed on sequences spanning 20 bp upstream and downstream of the circular DNA junction sites. The results showed that 45.84% of eccDNAs contained 4–20 bp direct repeat sequences, whereas 42.02% of eccDNAs contained inverted repeat sequences (Fig. 6C). Similarly, 43.48% of ecDNAs harbored 4–20 bp direct repeat sequences, while 40.87% contained inverted repeat sequences **(Supplementary Fig. 3C)**..

3.7 GC content analysis of EccDNAs/EcDNAs

GC content serves as a crucial indicator for understanding the structural-functional relationship of eccDNAs/ecDNAs. It influences the stability, secondary structure, and flexibility of eccDNAs/ecDNAs, thereby regulating gene expression, replication, and transcription efficiency. Additionally, GC content is closely associated with evolutionary adaptability and disease relevance. To further investigate the structure-function relationship of eccDNAs/ecDNAs, we analyzed their GC content. Results revealed no significant differences in GC content between ecDNAs ($P = 0.06$) (Fig. 6D) and eccDNAs ($P = 0.94$) **(Supplementary Fig. 3D)** in either the PCOS group or the control group.

3.8 Functional Analysis of eccDNAs and ecDNAs

To explore the biological functions of eccDNAs/ecDNAs and their molecular mechanisms in regulating the pathological progression of PCOS, we performed GO and KEGG enrichment analyses of genes carried by DEEECs/DEECs. In the biological process category, the top three enriched terms were cell junction assembly, intracellular sequestering of iron ions, and sequestering of iron ions. In the cellular component category, the top three terms were postsynaptic density, neuron-to-neuron synapse, and asymmetric synapse. In the molecular function category, the leading terms included odorant binding, cysteine-type endopeptidase inhibitor activity, and ferric iron binding (Fig. 7A, B). KEGG pathway analysis further revealed that these genes were significantly enriched in the T cell receptor signaling pathway (Fig. 7C, D).

To investigate the role of ecDNAs/eccDNAs in gene expression regulation, we compared the overlapping genes carried by eccDNAs between the two groups. The results showed high genomic dynamism, with 42.15% (6313/14,977) of eccDNAs covering partial gene fragments, and 78.26% (180/230) of ecDNAs encompassing more than one complete gene **(Supplementary Data 1)**. Specifically, 6,313 unique

eccDNAs overlapped with 4,101 genes, while 180 unique ecDNAs overlapped with 26,302 genes. Interestingly, many ecDNAs carried multiple genes, forming large “super ecDNAs” (e.g., ecDNAs(chr1:6993392–280850729) carrying 4,063 genes) **(Supplementary Data 1)**.

In addition, some genes showed a strong preference for circularization. Specifically, 6.53% (268/4,101) of host genes derived from eccDNAs were localized to more than three eccDNAs, while 36.26% (9,538/26,302) of host genes derived from ecDNAs exhibited a similar profile **(Supplementary Data 2)**. Notably, several “super genes” were positioned on circular DNAs; for instance, Camta1 formed 14 different eccDNAs and was detected in all six samples **(Supplementary Data 2)**..

3.9 The overlap between eccDNAs/ecDNAs and TEs, ncRNAs/circRNAs

Previous studies have shown that noncoding RNAs (ncRNAs) play crucial roles in PCOS(21), and their abnormal expression may lead to pathological changes such as disordered steroidogenesis, adipocyte dysfunction, and altered proliferation or apoptosis of ovarian cells(21, 22). Moreover, eccDNAs/ecDNAs can be transcribed into functional ncRNAs, which in turn regulate gene expression and drive disease progression. To explore how eccDNAs/ecDNAs regulate the core pathological mechanisms of PCOS through ncRNAs, we compared their genomic coordinates using the R/Bioconductor GenomicRanges and SplicingTypesAnno packages. The results showed that 2.98% (447/14,977) of eccDNAs overlapped with 208 unique ncRNAs, 2.91% (436/14,977) overlapped with 195 unique lncRNAs, and 0.08% (13/14,977) overlapped with 13 unique snoRNAs, while no overlap was found with tRNAs. Similarly, 81.30% (187/230) of ecDNAs overlapped with 4,210 unique ncRNAs, 81.30% (187/230) overlapped with 2,958 unique lncRNAs, 61.30% (141/230) overlapped with 1,357 unique snoRNAs, and 4.78% (11/230) overlapped with 5 unique tRNAs **(Supplementary Data 3–6)**. These findings indicate that eccDNAs/ecDNAs may exert biological functions through multiple types of ncRNAs, including lncRNAs, tRNAs, and snoRNAs.

Furthermore, Lanciano et al. reported that eccDNAs/EcDNAs are associated with the activity of transposable elements (TEs)(23, 24). TEs are mobile DNA sequences composed of repetitive elements that may contribute to the formation of eccDNAs/ecDNAs and influence tumor evolution and genetic diversity(25, 26). To further investigate, we compared the genomic coordinates of eccDNAs/ecDNAs with those of TEs. We found that 58.47% (8,757/14,977) of eccDNAs overlapped with 57,125 TEs, and 99.57% (229/230) of ecDNAs overlapped with 3,724 TEs **(Supplementary Data 7)**.

Iparraguirre et al. suggested that circular DNAs may generate transcripts similar to circRNAs. Accordingly, we compared the genomic coordinates of eccDNAs/ecDNAs with circRNA sequences obtained from the circBase database. The results showed that 25,080 circular RNAs overlapped partially or completely with 207 circular DNAs. Specifically, 1,276 eccDNAs overlapped with 1,544 circRNAs, while 207 ecDNAs overlapped with 23,536 circRNAs **(Supplementary Data 8).**.

3.10 Experimental Validation

Transmission electron microscopy confirmed the presence of ring-shaped eccDNA structures in both control and PCOS ovarian tissues, as visualized in representative sections (Fig. 8A). Consistent with these observations, PCR amplification using outward-facing primers yielded clear single bands at the expected sizes in both groups, indicating successful enrichment and specific amplification of circular DNA molecules. Notably, differences in band intensity were observed between control and PCOS samples, suggesting altered abundance of these eccDNAs. These changes were in agreement with the sequencing-based results. Quantitative analysis further demonstrated that eccDNA001, eccDNA002, and eccDNA004 were significantly decreased in the PCOS group, whereas eccDNA003 was markedly increased compared with controls (Fig. 8B).

4. Discussion

This study aims to investigate the sources and characteristics of ectopically expressed eccDNAs/ecDNAs in ovarian tissues from PCOS and control groups, and further explore their potential impact on the pathogenesis and progression of PCOS. we described the landscapes of eccDNAs/ecDNAs in ovary tissues of normal and PCOS by the circle-seq technique and investigated their characteristicsand formation mechanisms in detail (Fig. 9). Our findings reveal widespread expression of eccDNAs/ecDNAs in ovaries, exhibiting significant heterogeneity between the PCOS and control groups. Substantial differences exist between the two groups in terms of eccDNAs/ecDNAs quantity, length, and genomic origin. EccDNAs/EcDNAs may regulate PCOS development through the T cell receptor signaling pathway. This study is the first to reveal the expression profile of ecDNAs/ecDNAs in ovarian tissue from PCOS patients, which is of great significance for further analysis of the regulatory mechanisms of eccDNAs/ecDNAs in PCOS pathogenesis.

We found that the expression profile of eccDNAs/ecDNAs in PCOS ovarian tissue differed significantly from that in the control group, consistent with previous reports on human normal and FGR placentas(19), both showing markedly distinct expression patterns between disease and normal groups. Furthermore, we observed that both the quantity and diversity of eccDNAs/ecDNAs in the PCOS group were significantly lower than in the control group. Tingting Zhou et al. observed that in bone tissue from AIONFH, the number of ecDNAs in the AIONFH group (n = 88,720) was significantly lower than that in the control group (n = 596,621), a quantitative feature similar to our findings(27).

Research indicates that DNA-PK or PARP1 promotes ecDNAs formation, whereas elevated androgen levels suppress the activity of NHEJ-related enzymes such as DNA-PK or PARP1. Therefore, we hypothesize that the reduced eccDNAs/ecDNAs ratio in the PCOS group may result from PCOS-induced androgen suppression inhibiting the activity of NHEJ-related enzymes like DNA-PK or PARP1.

We found that the average length of eccDNA/EcDNA in the control group was significantly longer than that in the PCOS group. This phenomenon may stem from differences in DNA damage burden and repair mechanisms between the PCOS and control groups. In PCOS, chronic inflammation and oxidative stress impose a high DNA damage burden, compelling cells to favor faster but error-prone repair pathways

such as MMEJ or "imprecise" NHEJ. These pathways often involve more extensive resection of DNA ends and rely on short microhomologous sequences for ligation, thereby more readily generating shorter eccDNA fragments. In contrast, cells in the control group are in a more stable physiological state with a lower damage burden, allowing greater opportunity to employ more precise repair mechanisms (e.g., homologous recombination) or to retain longer DNA fragments during aberrant repair events before circularization. Consequently, eccDNAs formed in the control group exhibit a longer average length. This suppression reduces the cyclization process, leading to decreased eccDNAs levels.

From the perspective of chromosomal distribution, the chromosomal origin of eccDNAs/ecDNAs in the PCOS group was significantly different from that in the control group. Both groups had eccDNAs primarily derived from autosomes, a finding that was verified by the statistical results of eccDNAs density distribution per megabase. This is likely due to the genomic structure, replication, and transcription activities of sex chromosomes, which make them relatively stable in cells. As a result, sex chromosomes are less prone to abnormalities such as breakage and incorrect ligation during cellular physiological processes (unlike autosomes), leading to a smaller number of eccDNAs produced(28, 29).

Furthermore, we found that chromosome 1 in both groups produced a greater quantity and variety of eccDNAs/ecDNAs. We speculate that this phenomenon may reflect the intrinsic characteristics of the human genome, rather than a disease-specific mechanism. Qingrun Zhu et al. found that chromosome 19 contained more ecDNAs than any other chromosome in calcified bone tissue(18), while Huan Yang et al. discovered that chromosome 17 had more ecDNAs in the placenta(19). Chromosome 1 serves as the primary source of eccDNA, due to a combination of its inherent genomic characteristics, the pathological environment of PCOS, and the enrichment of risk genes on this chromosome. This may represent a potential molecular mechanism underlying PCOS.

These results indicate that the origin of eccDNAs/ecDNAs has a disease preference. To further understand the potential formation mechanism of eccDNAs/ecDNAs, we explored the nucleotide patterns around their junction sites. Our results revealed that at the junctions of eccDNAs/ecDNAs, there are not only direct repeat sequences but also a large number of inverted repeat sequences. Studies have shown that direct repeat sequences may be involved in the slippage mechanism during DNA replication, contributing to the formation of circular DNA. In contrast, inverted repeat sequences may be associated with DNA recombination and repair processes. For example, during chromosome division, large-scale breakage and random reconnection of chromosomal DNA can generate eccDNAs containing inverted repeat sequences.

Therefore, we speculate that the direct and inverted repeat sequences within 20 bp upstream and downstream of the junction sites may be involved in the formation of eccDNAs(24).

To investigate the biological functions of DEEECs/DEECs, we performed GO analysis on their host genes. The results revealed that host genes of DEEECs predominantly clustered in immune-related cellular components, biological processes, and functions. KEGG pathway enrichment analysis indicated that host genes of DEEECs/DEECs were enriched in the T cell receptor signaling pathway, a key pathway

involved in immune responses. Its activation involves TCR binding to antigen-peptide-MHC complexes, phosphorylation of Lck and ZAP-70, and subsequent downstream signaling. These activated pathways can trigger cytokine release and apoptosis, thereby affecting ovarian function. In PCOS, abnormal activation of the TCR signaling pathway may lead to chronic inflammation and immune dysregulation. Chronic inflammation can directly damage ovarian cells, suppress granulosa cell function, and impair normal follicular development and ovulation.

Additionally, inflammatory mediators such as TNF-α can interfere with insulin signaling pathways, exacerbating insulin resistance—a core feature of PCOS—which further promotes hyperandrogenism and ovarian dysfunction. EccDNA can activate innate immune responses by inducing type I interferon production through the cGAS-STING pathway. Simultaneously, eccDNA can activate adaptive immune responses by interacting with the TCR signaling pathway, promoting T cell activation and proliferation.

This chronic inflammation not only directly damages ovarian cells but also promotes hyperandrogenism, disrupts immune tolerance, and allows persistent activation of autoreactive T cells. This creates a vicious cycle that further exacerbates ovarian dysfunction and the pathological process of PCOS.

Our findings indicate that 58.47% of eccDNA and 99.57% of ecDNA in ovarian tissue overlap with transposable elements (TEs). TEs constitute a significant portion of eukaryotic genomes, accounting for approximately 44% of the human genome(30). TEs can move and replicate within genomes, and their abnormal expression and activity may lead to genomic structural alterations such as gene insertion, deletion, or rearrangement(31). These changes can directly or indirectly cause chromosomal breaks, resulting in the formation of eccDNA. Simultaneously, regulatory elements carried by TEs can integrate into eccDNA. If eccDNA carrying regulatory elements from TEs migrates near genes controlling androgen synthesis (e.g., CYP17A1, CYP11A1), it may drive these genes, causing ovarian cells to overproduce androgens, leading to hyperandrogenism.

We hypothesize that TEs may influence eccDNA generation through the aforementioned processes, with eccDNA subsequently affecting ovarian physiology and contributing to PCOS pathogenesis(32).

To further explore other potential functions of eccDNA/ecDNA, we compared its relationship with non-coding RNAs (ncRNAs). Results indicate that sequences of lncRNA, tRNA, circRNA, and snoRNA partially or completely overlap with ecDNA. In our findings, lncRNA uniquely overlaps with eccDNA/ecDNA. LncRNAs are extensively involved in crucial regulatory processes, including chromosomal silencing, genomic imprinting, chromatin modification, transcriptional activation, transcriptional interference, and nuclear transport(33). Furthermore, studies have reported the pivotal role of lncRNAs in polycystic ovary syndrome (PCOS)(34).

Mixue Tu et al. analyzed lncRNAs in PCOS, demonstrating that they primarily exert molecular effects by acting as competitive endogenous RNAs (ceRNAs) and showing significant correlations with several clinical phenotypes(35). These findings suggest that lncRNAs may serve as potential biomarkers for future investigations into the pathogenesis and development of follicular quality and function in PCOS

patients. Therefore, we hypothesize that eccDNA/ecDNA participates in the pathogenesis of PCOS through similar mechanisms.

In our findings, tRNA sequences overlap with ecDNA sequences but do not overlap with eccDNA sequences. The primary function of tRNA is to decode mRNA sequences and transport specific amino acids from aminoacyl-tRNA synthetases (AARs) to the ribosome(36). Beyond its classical role in protein translation, tRNA actively participates in other biological processes, such as initiating reverse transcription of retroviral genomes(37). However, no studies have directly linked tRNA to polycystic ovary syndrome (PCOS) to date. This suggests that ecDNA may influence tRNA metabolic pathways within cells—such as protein synthesis and amino acid biosynthesis—thereby impacting PCOS pathogenesis. For instance, tRNA abnormalities may disrupt amino acid metabolism, affecting hormone synthesis and cellular signaling pathways potentially relevant to PCOS pathophysiology(38). Consequently, elucidating how ecDNA mediates PCOS pathogenesis via tRNA could become a key research focus in future studies.

In our findings, 1,276 eccDNAs overlapped with 1,544 circRNAs, while 207 ecDNAs overlapped with 23,536 circRNAs. CircRNAs, as a form of circular DNA, have demonstrated potential roles in PCOS research. Iparraguirre et al. proposed that circular DNA may form transcripts similar to circRNAs(39). Yang Huan et al. compared the sequences of all eccDNAs/ecDNAs with data downloaded from the circBase database, subsequently identifying 11,148 circRNAs partially or fully overlapping with circular DNA segments. They proposed that eccDNAs/ecDNAs may influence disease pathogenesis by directly transcribing circRNAs(19).

CircRNAs play a role in PCOS progression by regulating multiple biological functions, including cell proliferation, apoptosis, and steroidogenesis(40). Jenan Sh. Nasser et al. discussed the roles of miRNAs, long non-coding RNAs, and circRNAs in PCOS pathogenesis(41), highlighting their potential as diagnostic biomarkers and therapeutic targets for PCOS(42).

Our findings reveal that snoRNAs exhibit varying degrees of overlap with eccDNA/ecDNAs, potentially influencing the expression or function of host genes and thereby participating in gene expression regulatory networks. SnoRNA is a type of non-coding RNA widely present in the nucleoli of eukaryotic cells. SnoRNAs participate in 2'-O-methylation and pseudo glycosylation modifications of rRNA, RNA processing, mRNA splicing, chromatin maintenance, and RNA editing(43). Additionally, they modify tRNA and mRNA and play roles in tumorigenesis and progression(44). Furthermore, snoRNAs enhance the stability of lncRNAs and maintain subcellular localization by forming snoRNA-lncRNA complexes(45). Complex interactions between lncRNAs and ecDNAs/ecDNAs may exist in gene expression regulation and cancer developmen(46). Research by Huang et al.indicates that certain ecDNA sites in the genome highly overlap with snoRNA family members, suggesting that these snoRNAs function in gene expression. However, no studies have yet identified direct relationships between ecDNA and snoRNA. Whether ecDNA/ecDNAs can mediate polycystic ovary syndrome (PCOS) progression by altering snoRNA expression remains an intriguing area for future research.

In summary, eccDNAs/ecDNAs show tremendous promise in the diagnosis and prognosis of various diseases, including cancer. Among these applications, eccDNAs/ecDNAs analysis is widely used in prenatal screening for trisomy syndromes, demonstrating exceptionally high accuracy(47). Current research on eccDNA/ecDNAs primarily focuses on its potential in cancer diagnosis and prognosis, as well as advancements in ecDNA detection technologies, without directly addressing its application in PCOS screening. Our study employs circulating-sequencing technology to reveal differences in ecDNA expression between normal ovarian tissue and PCOS ovarian tissue, delving into their specific characteristics and formation mechanisms (see Fig. 9). Findings suggest that ecDNA may exert a potential driving role in PCOS through immune signaling pathways.

Furthermore, we observed substantial genomic annotation overlap between numerous ncRNAs and eccDNA/ecDNAs, indicating complex interactions and biological functions between them. Compared to linear DNA, ecDNA/EcDNAs exhibit greater stability, which confers potential as biomarkers. Targeted interventions against eccDNA/ecDNAs may hold therapeutic value in clinical settings. Moreover, in current cancer-related gene studies, monitoring eccDNA/ecDNAs could serve as a target for evaluating therapeutic efficacy. These findings may aid in the development of a novel non-invasive diagnostic tool tailored for polycystic ovary syndrome (PCOS). Therefore, utilizing eccDNA/ecDNAs as biomarkers for PCOS holds significant clinical value. Despite the innovative nature of these discoveries, the specific functions of circular DNA require further investigation to fully unravel its mysteries.

Abbreviations

PCOS
Polycystic Ovary Syndrome
eccDNAs/ecDNAs
Extrachromosomal Circular DNA
DHEA
Dehydroepiandrosterone
ELISA
Enzyme-Linked Immunosorbent Assay
GO
Gene Ontology
KEGG
Kyoto Encyclopedia of Genes and Genomes
TEM
Transmission Electron Microscopy
DEEECs/DEECs
Differentially Expressed eccDNAs/ecDNAs
ncRNAs
Non-Coding RNAs
TEs

Transposable Elements
circRNAs
Circular RNAs
LH
Luteinizing Hormone
BPA
Bisphenol A
MMEJ
Minor-Homologous End Joining
NHEJ
Non-Homologous End Joining
AIONFH
Alcohol-Induced Osteonecrosis of The Femoral Head
H&E
Hematoxylin and Eosin
FSH
Follicle-Stimulating Hormone
HMW
High Molecular Weight
PCA
Principal Component Analysis
UCSC
University of California, Santa Cruz
DNA-PK
DNA-Dependent Protein Kinase
PARP1
Poly ADP-Ribose Polymerase 1

Declarations

Funding Statement: This study was supported by the National Natural Science Youth Foundation (Approval No.82205177\82301905), Chongqing Natural Science Foundation (No.2024NSCQ-MSX2667) and The program of Inheritance and Innovation of Traditional Chinese Medicine in Chongqing (Chongqing Traditional Chinese Medicine (2022) No.33).These funder had role in study design, data collection and analysis, decision to publish, or preparation of the manuscript.

Disclosure Statement: The authors declare that they have no known competing financial interests or personal relationships that could have appeared to influence the work reported in this paper.

Attestation Statement:

Data regarding any of the subjects in the study has not been previously published unless specified.

Data will be made available to the editors of the journal for review or query upon request.

Data Sharing Statement:

Individual de-identified participant data (including data dictionaries) will be shared. The study protocol and statistical analysis plan are available upon request. Data will be available beginning 9 months and ending 36 months following article publication. Researchers who provide a methodologically sound proposal may apply for data access. Proposals should be directed to 1050578533@qq.com.

Capsule: This study first characterizes the extrachromosomal circular DNA expression profile in PCOS ovaries, revealing reduced abundance, altered length distribution, and functional involvement in synaptic structure, signal transmission, and T cell receptor signaling.

Author Contribution

Zhi Chen: Conceptualization, Methodology, Formal analysis, Investigation, Data curation, Writing – original draft, Writing – review & editing, Supervision, Project administration, Funding acquisition.Hao Song: Writing – original draft.Jun-jie Deng: Methodology,Data curation,.Yuan-xue Wu: Investigation.Tian-jiao Liu: Resources, Data curation.Min Xia<sup>: Conceptualization, Methodology, Supervision.Ao-lei Lin<sup>: Writing – review & editing.Cheng Chen<sup>: Resources.Jun-yu Feng<sup>: Writing – review & editing.Huan Yang: Conceptualization, Methodology, Resources, Writing – review & editing, Supervision, Project administration, Funding acquisition.

Declaration of competing interest

The authors declare that they have no known competing financial interests or personal relationships that could have appeared to influence the work reported in this paper.

Acknowledgements

The authors thank Shanghai NewCore Biotechnology for bioinformatics data analysis support.

Supplementary Material

The National Center for Biotechnology Information supporting the findings of this study is available in the National Center for Biotechnology Information under the number PRJNA1198481 (www.ncbi.nlm.nih.gov/sra/PRJNA1198481).

References

1. Chang K-J, Chen J-H, Chen K-H. The Pathophysiological Mechanism and Clinical Treatment of Polycystic Ovary Syndrome: A Molecular and Cellular Review of the Literature. Int J Mol Sci. 2024;25(16):9037.
2. Sadeghi HM, Adeli I, Calina D, Docea AO, Mousavi T, Daniali M, et al. Polycystic Ovary Syndrome: A Comprehensive Review of Pathogenesis, Management, and Drug Repurposing. Int J Mol Sci. 2022;23(2):583.
3. Goh JE, Farrukh MJ, Keshavarzi F, Yap CS, Saleem Z, Salman M, et al. Assessment of prevalence, knowledge of polycystic ovary syndrome and health-related practices among women in klang valley: A cross-sectional survey. Front Endocrinol. 2022;13:985588.
4. Deswal R, Narwal V, Dang A, Pundir CS. The prevalence of polycystic ovary syndrome: a brief systematic review. J Hum Reprod Sci. 2020;13(4):261–71.
5. Cai M, Ni Z, Yuan Z, Yu J, Zhang D, Yao R, et al. Past and present: a bibliometric study on polycystic ovary syndrome. J Ovarian Res. 2023;16(1):42.
6. Rosenfield RL, Ehrmann DA. The Pathogenesis of Polycystic Ovary Syndrome (PCOS): The Hypothesis of PCOS as Functional Ovarian Hyperandrogenism Revisited. Endocr Rev. 2016;37(5):467–520.
7. Meier RK. Polycystic ovary syndrome. Nurs Clin North Am. 2018;53(3):407–20.
8. Gaubatz JW. Extrachromosomal circular DNAs and genomic sequence plasticity in eukaryotic cells. Mutat Res. 1990;237(5–6):271–92.
9. Lu B, Winnall S, Cross W, Barnes CP. Cell-cycle dependent DNA repair and replication unifies patterns of chromosome instability. Nat Commun. 2025;16(1):3033.
10. Li F, Ming W, Lu W, Wang Y, Dong X, Bai Y. Bioinformatics advances in eccDNA identification and analysis. Oncogene. 2024;43(41):3021–36.
11. Zhong T, Wang W, Liu H, Zeng M, Zhao X, Guo Z. eccDNA atlas: a comprehensive resource of eccDNA catalog. Briefings Bioinf. 2023;24(2):bbad037.
12. Arrey G, Keating ST, Regenberg B. A unifying model for extrachromosomal circular DNA load in eukaryotic cells. Semin Cell Dev Biol. 2022;128:40–50.
13. Luebeck J, Ng AWT, Galipeau PC, Li X, Sanchez CA, Katz-Summercorn AC, et al. Extrachromosomal DNA in the cancerous transformation of barrett's oesophagus. Nature. 2023;616(7958):798–805.
14. Huang Q, Zhang S, Wang G, Han J. Insight on ecDNA-mediated tumorigenesis and drug resistance. Heliyon. 2024;10(6):e27733.
15. Yan X, Mischel P, Chang H. Extrachromosomal DNA in cancer. Nat Rev Cancer. 2024;24(4):261–73.
16. Dong Y, He Q, Chen X, Yang F, He L, Zheng Y. Extrachromosomal DNA (ecDNA) in cancer: mechanisms, functions, and clinical implications. Front Oncol. 2023;13:1194405.
17. Paulsen T, Shibata Y, Kumar P, Dillon L, Dutta A. Small extrachromosomal circular DNAs, microDNA, produce short regulatory RNAs that suppress gene expression independent of canonical promoters. Nucleic Acids Res. 2019;47(9):4586–96.

18. Zhu Q, Chen R, Kuang M, Zhang W, Wang D, Han S. Identification and characterization of extrachromosomal circular DNA in age-related osteoporosis. Aging. 2023;15(24):15489–503.
19. Yang H, He J, Huang S, Yang H, Yi Q, Tao Y, et al. Identification and characterization of extrachromosomal circular DNA in human placentas with fetal growth restriction. Front Immunol. 2021;12:780779.
20. Yu G, Wang L-G, Han Y, He Q-Y. clusterProfiler: an R package for comparing biological themes among gene clusters. OMICS: J Integr Biol. 2012;16(5):284–7.
21. Mu L, Sun X, Tu M, Zhang D. Non-coding RNAs in polycystic ovary syndrome: a systematic review and meta-analysis. Reprod Biol Endocrinol: RB&E. 2021;19(1):10.
22. Møller HD, Bojsen RK, Tachibana C, Parsons L, Botstein D, Regenberg B. Genome-wide purification of extrachromosomal circular DNA from eukaryotic cells. J Vis Exp: JoVE. 2016;(110):e54239 |.
23. Lanciano S, Cristofari G. Measuring and interpreting transposable element expression. Nat Rev Genet. 2020;21(12):721–36.
24. Zhang P, Mbodj A, Soundiramourtty A, Llauro C, Ghesquière A, Ingouff M, et al. Extrachromosomal circular DNA and structural variants highlight genome instability in arabidopsis epigenetic mutants. Nat Commun. 2023;14(1):5236.
25. Conrad DF, Pinto D, Redon R, Feuk L, Gokcumen O, Zhang Y, et al. Origins and functional impact of copy number variation in the human genome. Nature. 2010;464(7289):704–12.
26. Turner KM, Deshpande V, Beyter D, Koga T, Rusert J, Lee C, et al. Extrachromosomal oncogene amplification drives tumour evolution and genetic heterogeneity. Nature. 2017;543(7643):122–5.
27. Zhou T, Ma S, Zhao Y, Guo D, Wang H, Kuang M, et al. Identification and characterization of extrachromosomal circular DNA in alcohol induced osteonecrosis of femoral head. Front Genet. 2022;13:918379.
28. Eugen-Olsen RAB, Hariprakash JM, Oestergaard VH, Regenberg B. Molecular mechanisms of extrachromosomal circular DNA formation. Nucleic Acids Res. 2025;53(5):gkaf122.
29. Wang Z, Yu J, Zhu W, Hong X, Xu Z, Mao S, et al. Unveiling the mysteries of extrachromosomal circular DNA: from generation to clinical relevance in human cancers and health. Mol Cancer. 2024;23(1):276.
30. Chénais B, Caruso A, Hiard S, Casse N. The impact of transposable elements on eukaryotic genomes: from genome size increase to genetic adaptation to stressful environments. Gene. 2012;509(1):7–15.
31. Wells JN, Feschotte C. A Field Guide to Eukaryotic Transposable Elements. Annu Rev Genet. 2020;54:539–61.
32. Li J, Chen H, Gou M, Tian C, Wang H, Song X, et al. Molecular Features of Polycystic Ovary Syndrome Revealed by Transcriptome Analysis of Oocytes and Cumulus Cells. Front Cell Dev Biol. 2021;9:735684.

33. Kopp F, Mendell JT. Functional classification and experimental dissection of long noncoding RNAs. Cell. 2018;172(3):393–407.
34. Xuan F, Jin R, Zhou W, Ye Y, Ren Y, Lu J, et al. LncRNA SNHG12 promotes cell proliferation and inhibits apoptosis of granulosa cells in polycystic ovarian syndrome by sponging miR-129 and miR-125b. J Ovarian Res. 2024;17(1):72.
35. Tu M, Wu Y, Mu L, Zhang D. Long non-coding RNAs: novel players in the pathogenesis of polycystic ovary syndrome. Ann Transl Med. 2021;9(2):173.
36. Schimmel P. The emerging complexity of the tRNA world: mammalian tRNAs beyond protein synthesis. Nat Rev Mol Cell Biol. 2018;19(1):45–58.
37. Orellana EA, Siegal E, Gregory RI. tRNA dysregulation and disease. Nat Rev Genet. 2022;23(11):651–64.
38. Chen M, Kato K, Kubo Y, Tanaka Y, Liu Y, Long F, et al. Structural basis for tRNA-dependent cysteine biosynthesis. Nat Commun. 2017;8(1):1521.
39. Iparraguirre L, Prada-Luengo I, Regenberg B, Otaegui D. To Be or not to Be: circular RNAs or mRNAs from circular DNAs? Front Genet. 2019;10:940.
40. Jing T, Wu Y, Wan A, Ge C, Chen Z-J, Du Y. Circular RNA as a novel regulator and promising biomarker in polycystic ovary syndrome. Biomolecules. 2023;13(7):1101.
41. Nasser JS, Altahoo N, Almosawi S, Alhermi A, Butler AE. The role of MicroRNA, long non-coding RNA and circular RNA in the pathogenesis of polycystic ovary syndrome: a literature review. Int J Mol Sci. 2024;25(2):903.
42. Yu L, Wang C, Zhang D, Liu M, Liu T, Pan B, et al. Exosomal circ_0008285 in follicle fluid regulates the lipid metabolism through the miR-4644/ LDLR axis in polycystic ovary syndrome. J Ovarian Res. 2023;16(1):113.
43. Grzechnik P, Szczepaniak SA, Dhir S, Pastucha A, Parslow H, Matuszek Z, et al. Nuclear fate of yeast snoRNA is determined by co-transcriptional Rnt1 cleavage. Nat Commun. 2018;9(1):1783.
44. Huang Z-H, Du Y-P, Wen J-T, Lu B-F, Zhao Y. snoRNAs: functions and mechanisms in biological processes, and roles in tumor pathophysiology. Cell Death Discovery. 2022;8(1):259.
45. Yin Q-F, Yang L, Zhang Y, Xiang J-F, Wu Y-W, Carmichael GG, et al. Long noncoding RNAs with snoRNA ends. Mol Cell. 2012;48(2):219–30.
46. Ransohoff JD, Wei Y, Khavari PA. The functions and unique features of long intergenic non-coding RNA. Nat Rev Mol Cell Biol. 2018;19(3):143–57.
47. Marton T, Erdélyi ZR, Takai M, Mészáros B, Supák D, Ács N, et al. Systematic Review of Accuracy Differences in NIPT Methods for Common Aneuploidy Screening. J Clin Med. 2025;14(8):2813.

Figures

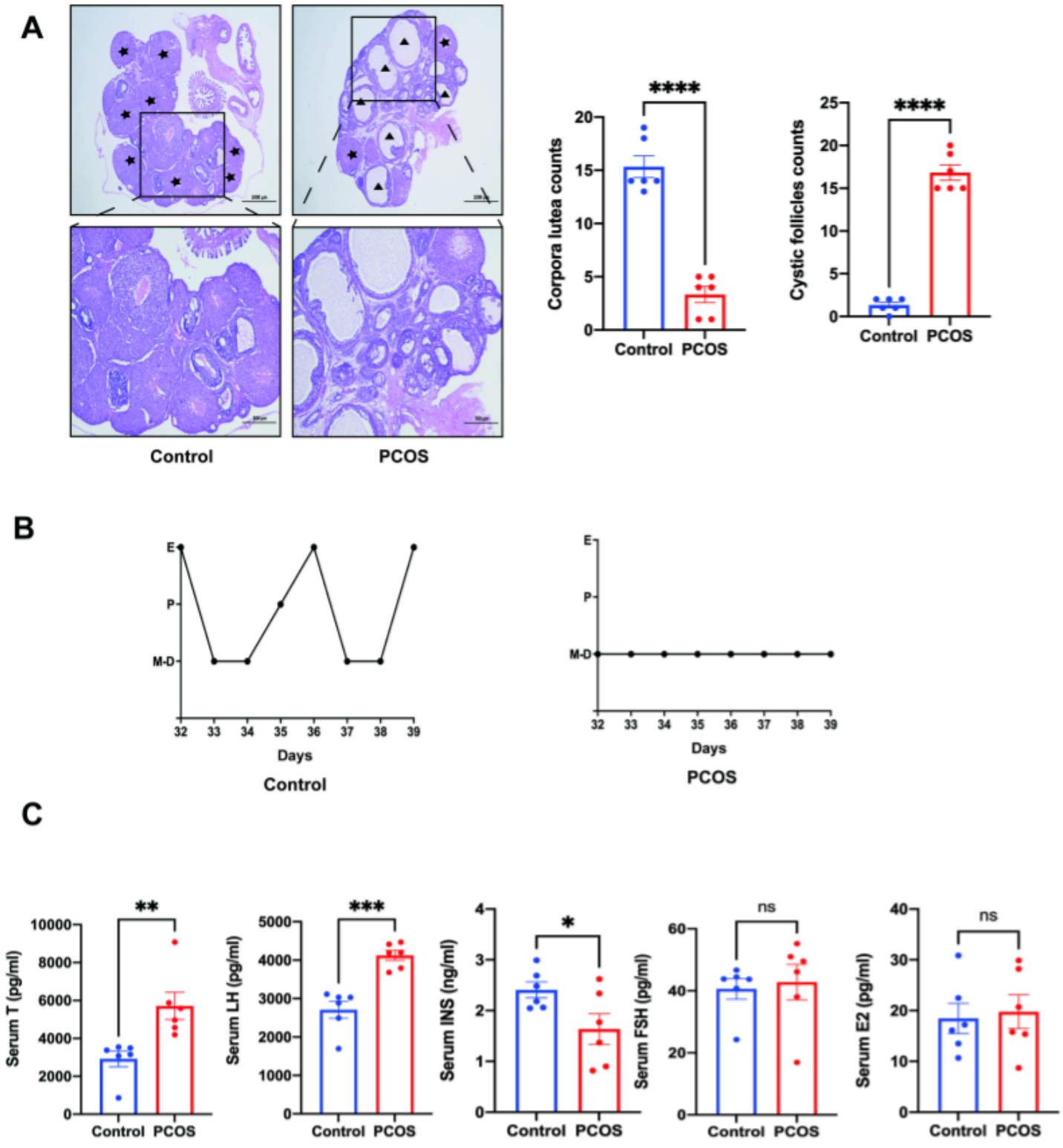

Figure 1

Establishment and validation of the PCOS rat model. (A) Representative hematoxylin and eosin–stained ovarian sections from control and PCOS rats. Control ovaries exhibit follicles at different developmental stages and abundant corpora lutea (▯), whereas PCOS ovaries display multiple cystic follicles (▲) with a marked reduction in corpora lutea. The boxed areas indicate regions shown at higher magnification below. Quantification of corpora lutea and cystic follicles is shown on the right. (B) Estrous cycle

monitoring over consecutive days showing regular cyclicity in control rats and persistent diestrus arrest in PCOS rats. (C) Serum hormone levels in control and PCOS rats, including testosterone (T), luteinizing hormone (LH), insulin (INS), follicle-stimulating hormone (FSH), and estradiol (E2). Data are presented as mean ± SEM. Statistical significance was determined by Student's t-test. $P < 0.05$, $P < 0.01$, $P < 0.001$, $P < 0.0001$; ns, not significant.

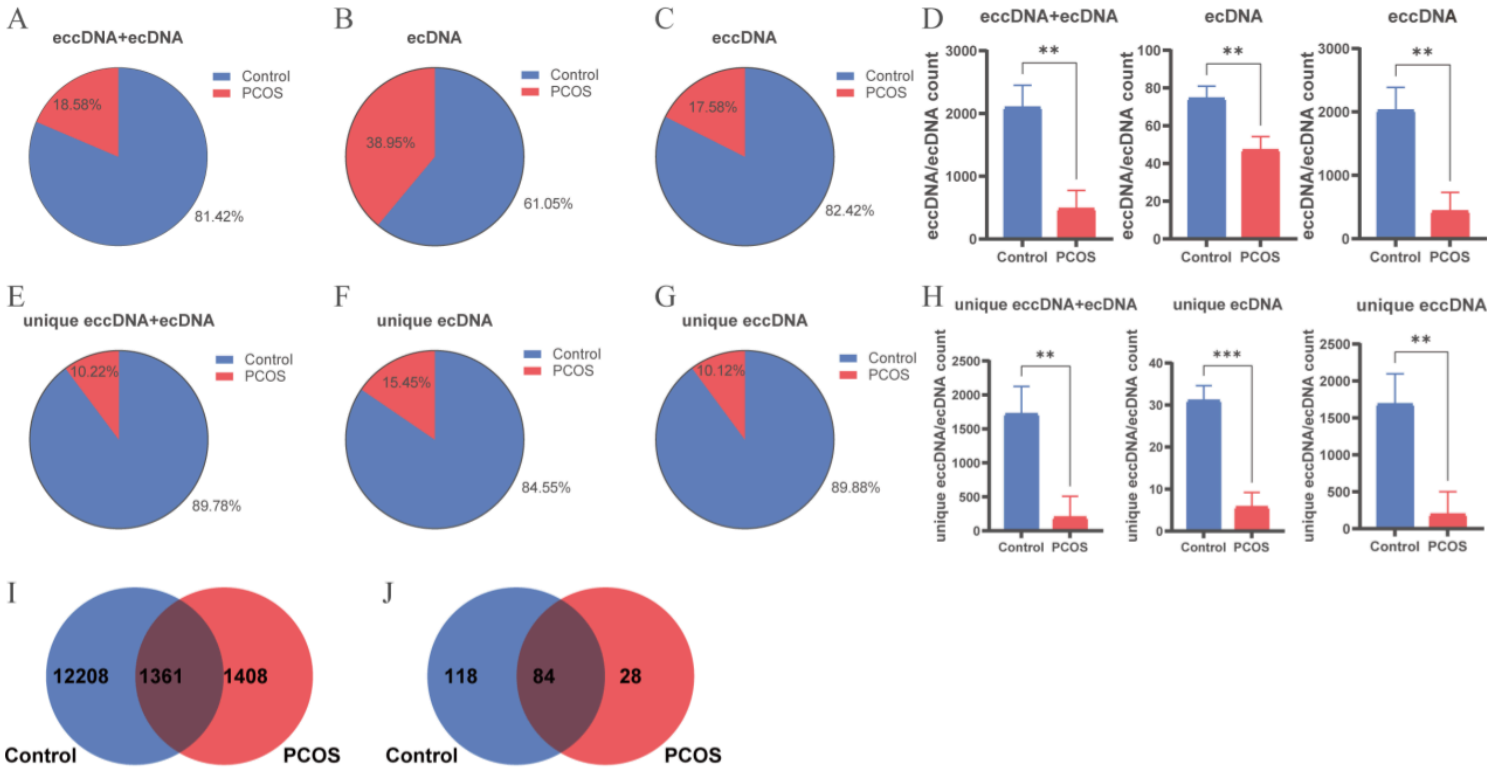

Figure 2

Quantitative statistics of eccDNAs/ecDNAs and Unique eccDNAs/ecDNAs in the control group and PCOS group. (A) Total number of eccDNAs/ecDNAs across both groups; (B) Total number of ecDNAs across both groups; (C) Total number of eccDNAs across both groups. (D) Analysis of the difference in eccDNAs/ecDNAs between the two groups. (E) Number of unique eccDNAs/ecDNAs in both groups. (E) Number of unique ecDNAs in both groups. (G) Number of unique eccDNAs in both groups. (H) Analysis of the difference in the number of unique eccDNAs/ecDNAs between the two groups. (I)eccDNAs are shared between PCOS and control groups.(J)eccDNAs are shared between PCOS and control groups.

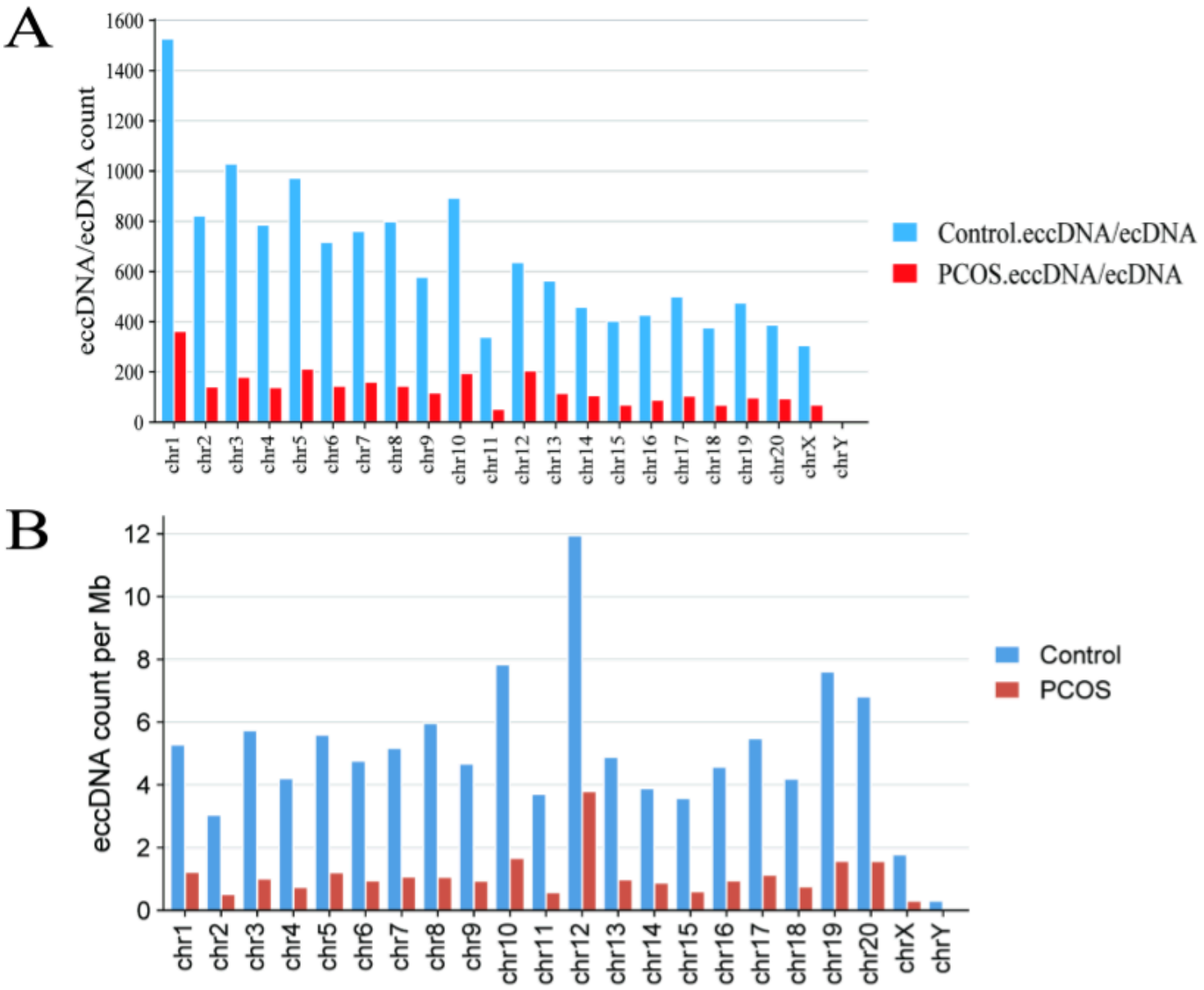

Figure 3

Chromosomal distribution of eccDNA/ecDNA in control and PCOS rats. (A) Quantitative distribution of eccDNAs/ecDNAs across different chromosomes. (B) Genome view of normalized eccDNA distribution in groups PCOS and control eccDNA counts per Mb are shown on the Y-axis.

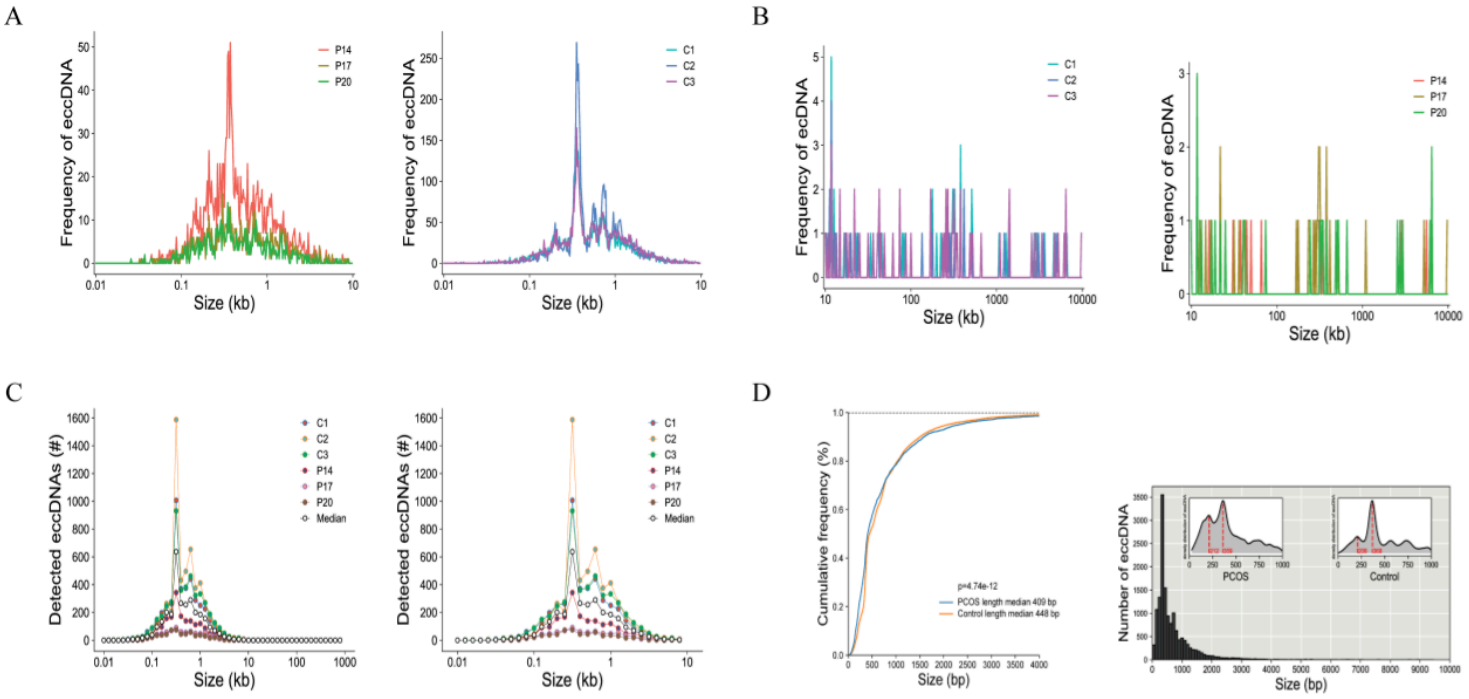

Figure 4

Size distribution of ovarial-derived eccDNAs/ecDNAs. (A) Size profiling of total eccDNAs in the ovary. (B) Size profiling of total ecDNAs in the ovary. (C) Size profiling of total eccDNAs/ecDNAs in the ovary. (D) Cumulative frequency plot of eccDNAs in PCOS and control ovary. Sizes were capped at 4000bp for both groups of molecules.The length density distribution of eccDNAs of PCOS and control groups. There are four peaks at 212 bp, 359 bp,208 bp, and 368 bp, respectively.

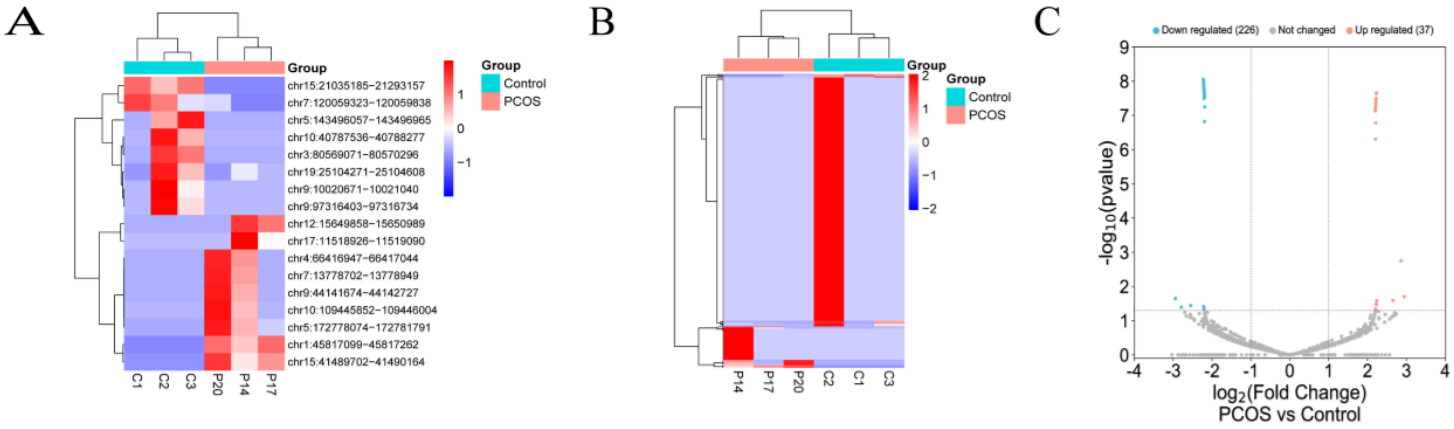

Figure 5

Correlation analysis between samples. (A□B□C) Cluster and volcano plots show eccDNAs differentially expressed in the OP group.

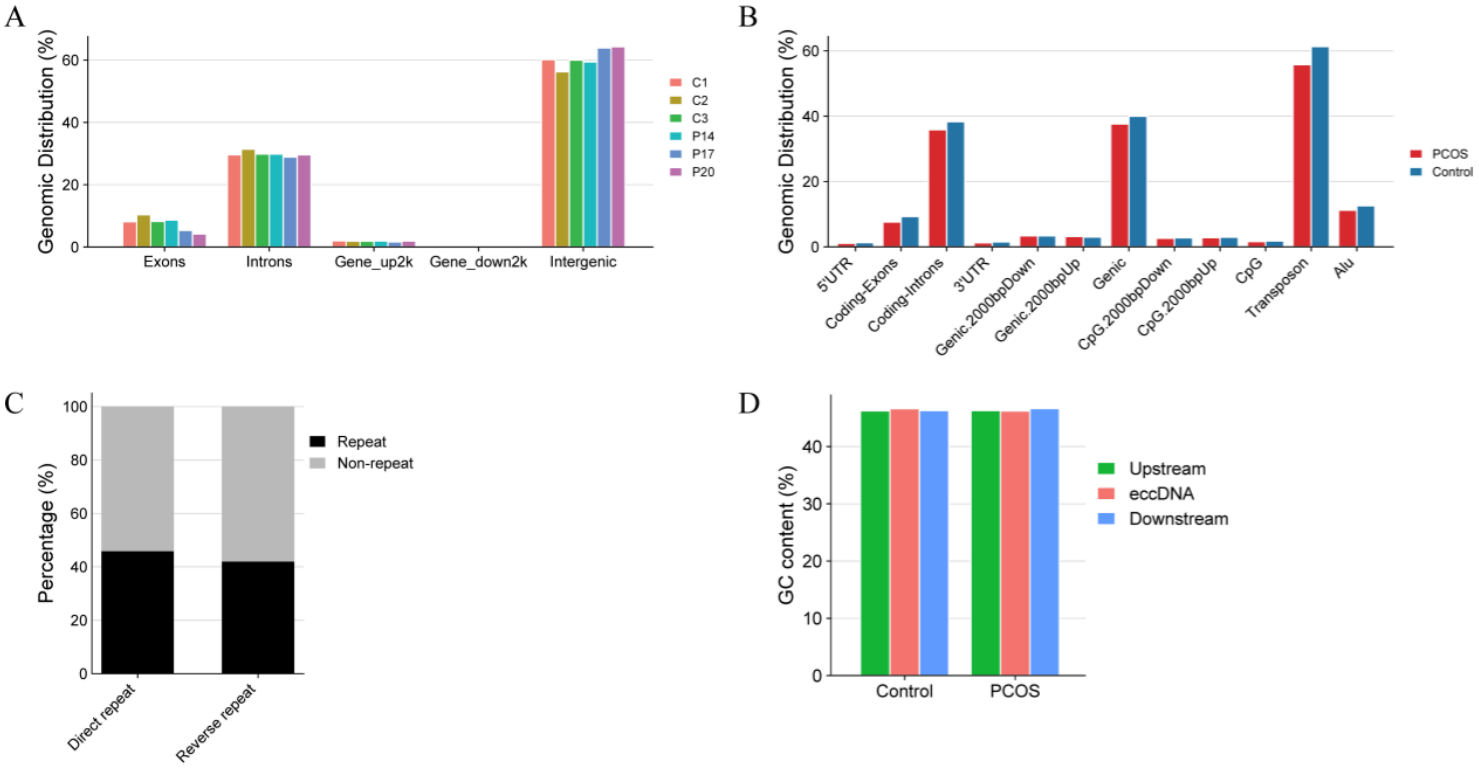

Figure 6

Properties of the loci that release eccDNAs. (A) The distribution of eccDNAs of each sample on whole-genome chromosome region. (B) Distribution of

eccDNAs of PCOS and normal groups in the indicated genomic region. (C) Percentage of eccDNAs with (black) or without (gray) 4~20bp direct or reverse repeats flanking junction locus at the genomic source. (D) Median percent GC content of eccDNAs and the genomic sequences of equal length upstream or downstream of the eccDNAs source loci.

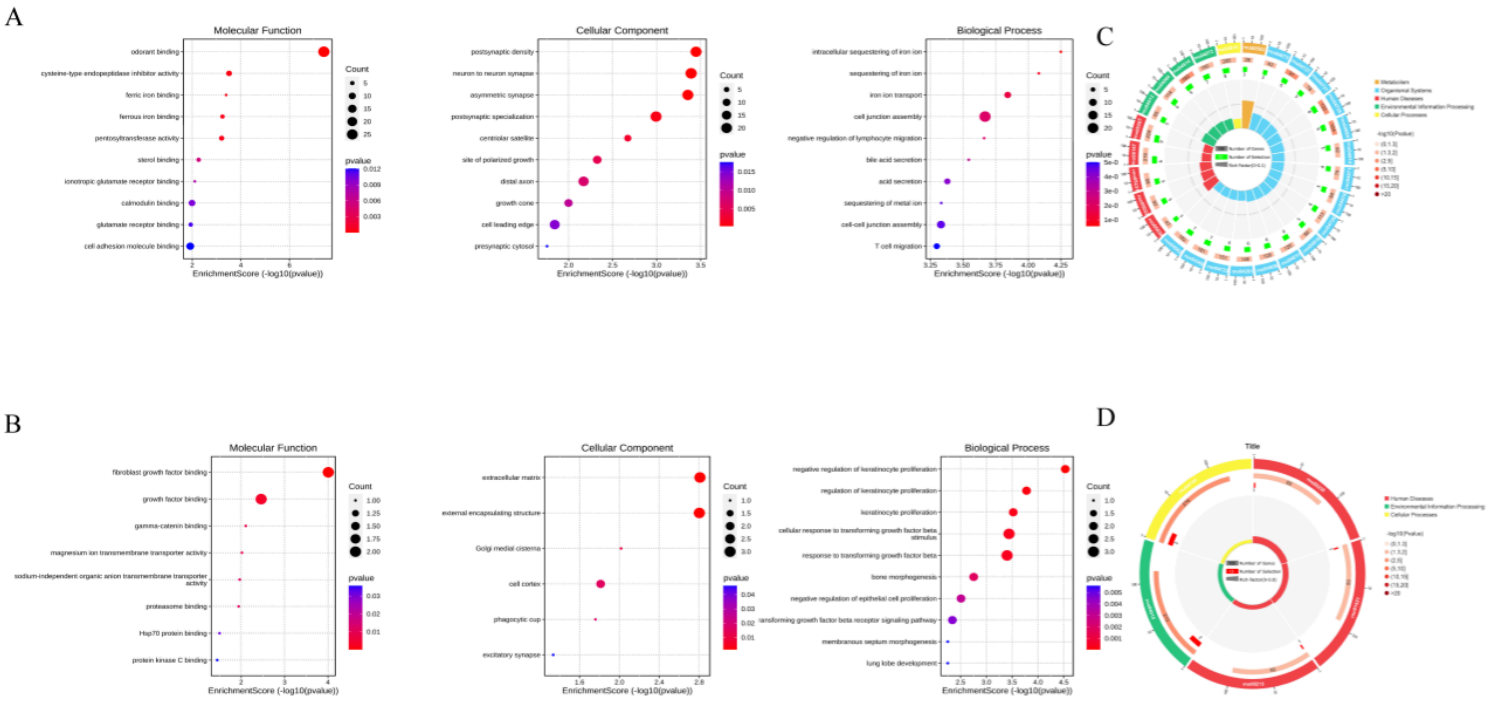

Figure 7

The enrichment map for differentially expressed host-genes on DEEECs/DEECs generated using GO and KEGG pathway analyses. (A) GO enrichment analyses of host-genes on DEEECs. (B) GO enrichment analyses of host-genes on DEECs. (C) KEGG enrichment analyses of host-genes on DEECs. (D) KEGG enrichment analyses of host-genes on DEEECs.

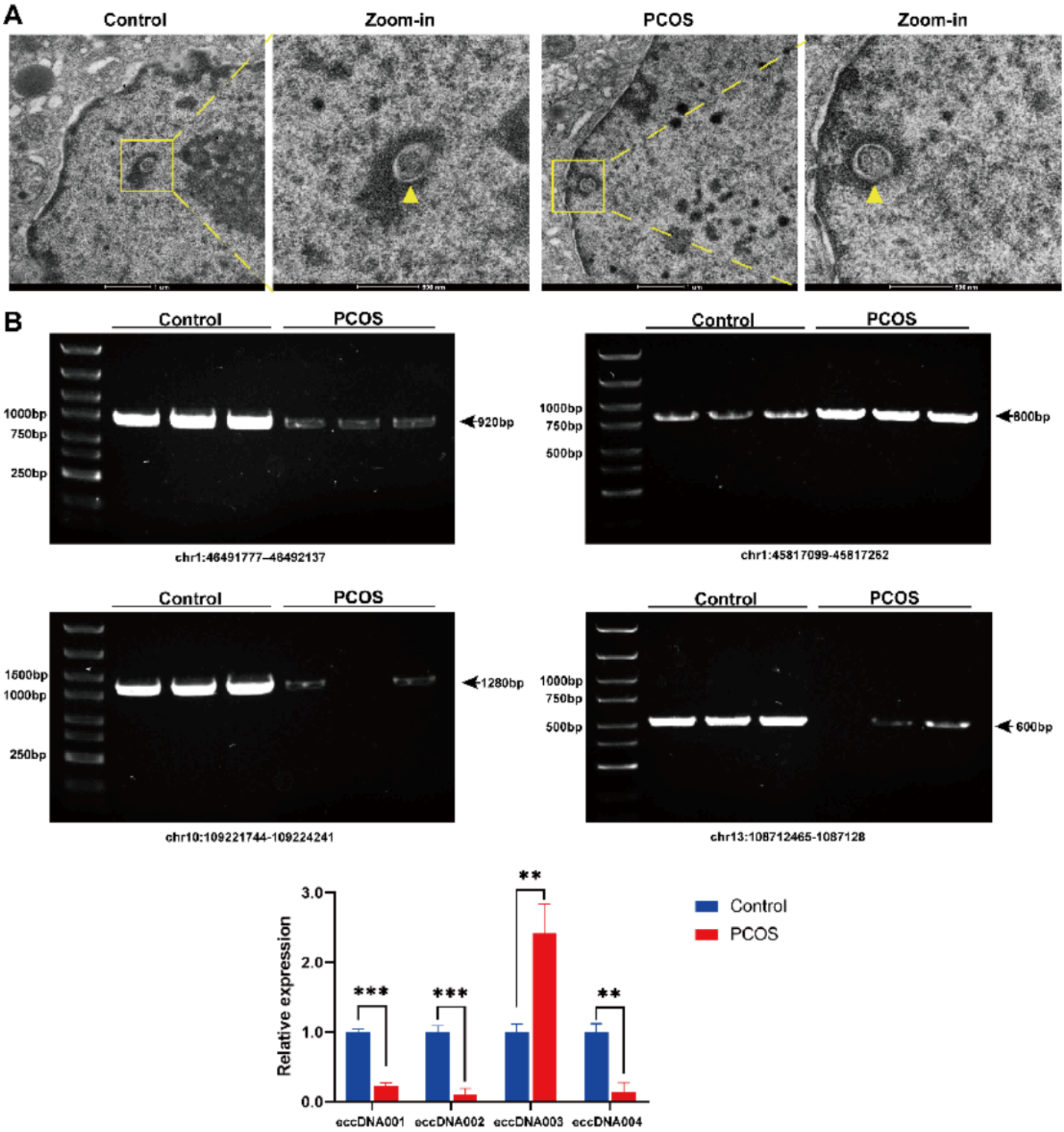

Figure 8

Ultrastructural and experimental validation of eccDNAs in rat ovaries. (A) Transmission electron microscopy images of ovarian tissues from control and PCOS rats. Yellow arrows indicate electron-dense circular DNA–like structures suggestive of eccDNAs, which were markedly increased in PCOS ovaries. Scale bar = 500 nm. (B) Agarose gel electrophoresis verification of eccDNA001–eccDNA004 amplified from ovarian tissues of control and PCOS rats.

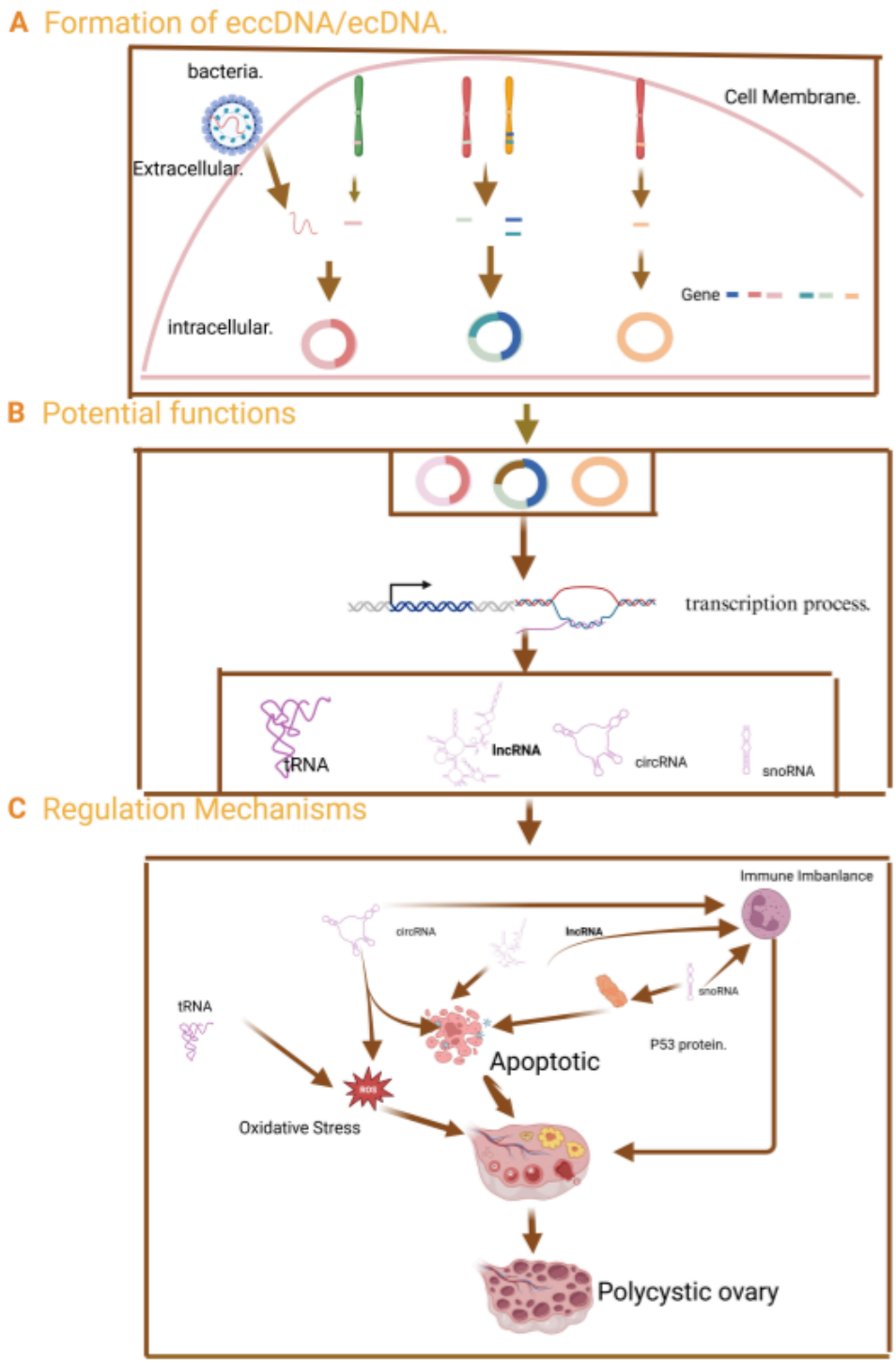

Figure 9

Schematic illustration of eccDNA/ecDNA formation and its regulatory mechanisms in polycystic ovary syndrome (PCOS). (A) Formation of eccDNA/ecDNA. Extracellular eccDNA/ecDNA originates from bacteria and enters cells through the cell membrane. Intracellularly, eccDNA/ecDNA can be generated from chromosomal DNA through various mechanisms, resulting in circular DNA molecules containing different gene fragments. (B) Potential functions. Once formed, eccDNA/ecDNA participates in the

transcription process, serving as templates for the generation of non-coding RNAs, including tRNA, lncRNA, circRNA, and snoRNA. (C) Regulation mechanisms. These eccDNA/ecDNA-derived non-coding RNAs contribute to PCOS pathogenesis through multiple pathways: tRNA and circRNA promote oxidative stress and apoptosis; lncRNA and snoRNA modulate P53 protein expression; and the collective effects of these molecular alterations ultimately lead to immune imbalance and the development of polycystic ovary characteristics.

Supplementary Files

This is a list of supplementary files associated with this preprint. Click to download.

- SupplementaryTable1.docx